

Date of publication xxxx 00, 0000, date of current version xxxx 00, 0000.

Digital Object Identifier 10.1109/ACCESS.2023.00000

# Multi-point Mapping of Dancer Aesthetic Movements Onto a Robotic Arm

GIUSEPPE SAVIANO<sup>1,2</sup>, (Student Member, IEEE), ALBERTO VILLANI<sup>1</sup>, (Student Member, IEEE), DOMENICO PRATTICHIZZO<sup>1,3</sup>, (Fellow, IEEE)

<sup>1</sup>Department of Information Engineering and Mathematics, University of Siena, Siena (e-mail: alberto.villani@unisi.it, dprattichizzo@unisi.it)

<sup>2</sup>Department of Computer Science, University of Pisa, Pisa (e-mail: giuseppe.saviano@phd.unipi.it)

<sup>3</sup>Department of Humanoids and Human Centered Mechatronics, Istituto Italiano di Tecnologia, Genova, Italy (e-mail: domenico.prattichizzo@iit.it)

**ABSTRACT** Dance and robotics share the investigation field of motion of articulated kinematic chains for aesthetic and practical purposes, respectively. The first researches the gracefulness of movements of the performer's body to express emotion and captivate audiences, while the latter focuses on planning and controlling the motion of mechanical systems to complete pragmatic tasks. However, in recent years, even more and more robots have stepped on stages together with artists and dancers with the aim of enchanting the spectators with original and groundbreaking choreographies.

In this study, we propose an approach to combine the graceful motion of a dancer with autonomous trajectory planning for an articulated arm in unique human-robot choreographies (HRCs). The expressiveness of dance and the posture of dancers are rendered in a robotic manipulator, mapping i) the most involved dancer limb and ii) the human center of gravity. The simultaneous mapping of these two points is achieved by exploiting the kinematic kernel of the redundant robot, by which it is possible to mime the dancer's posture while the end-effector follows the limb movements. In this way, we developed an autonomous human-to-robot mapping method for aesthetic purposes that balances dance expressiveness and dancer posture. To validate the proposed method, we compared robot control performance and movement coherence with human-originating dances against robot movements obtained by tracking single points. Additionally, the effects of the multi-point projection on the audience experience were evaluated in an experimental campaign involving 30 participants. Their feedback confirmed the paramount of using the human centroid and end limb to represent human posture and dance nuances, respectively, and the positive impact of simultaneous mapping of these points on the audience's experience.

**INDEX TERMS** Human-Robot Interaction (HRI), Human-Robot Choreography (HRC), Social Robots, Motion Mapping

## I. INTRODUCTION

DANCE is the artistic discipline aimed at expressing emotions and fascinating the audience using the harmonious movements of its actors, be they human or artificial. [1]. Recently, dance performances have been augmented by the synchronous movements of artifacts such as mirrors, light rays, morphing backgrounds, drones, and sometimes articulated robots including humanoids and manipulators. Pro dancers like Merritt Moore and Roberto Bolle offered to their audience choreographies where they interacted with moving robotic arms, staging a dialog between the human and the machine [2], [3]. Also, companies such as Boston Dynamics have become worldwide known for their captivating commercial and research featuring dancing robots [4]. However, according to publicly available interviews, the choreographed

movements of robots are previously planned or sometimes teleoperated [5], [6], lengthening the performance preparation time and reducing the improvisation creative space of artists. In this work, we present a novel approach to the autonomous creation of augmented aesthetic experiences involving humans and manipulators through multi-point mapping of dancer movements onto the robotic arm. Fig. 1 visually depicts the concept of this work.

### A. RELATED WORKS

Starting from the Eysenck theory [7] about objective parameters influencing the experience of a dance audience, several research teams investigated which motion features are correlated to the spectator's beauty perception. Torrents *et al.* in [8] and Neave *et al.* in [9] identified movements amplitude,

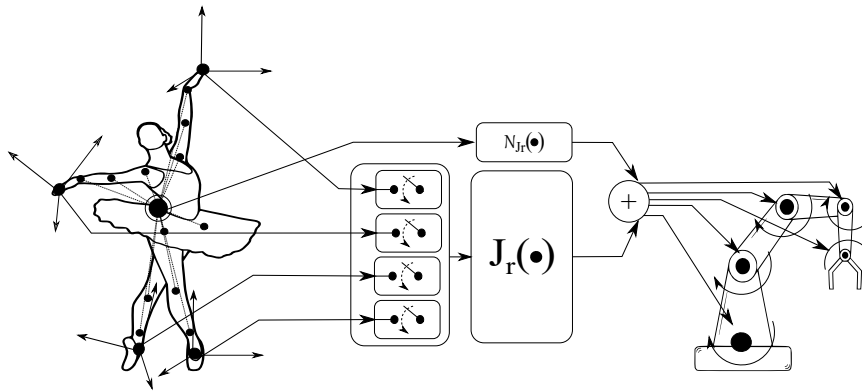


FIGURE 1: Schematic representation of the multi-point mapping of dancer movement onto robotic arm motion matching the position of the centers of gravity and the most variable end limb with the end-effector. According to a variance measure, one of the dancer's end limbs is exploited as a reference for robot end effector movements, while the human center of gravity is used to set the position of the robot geometrical one. The tracking of the end-limb and centroid are the primary and secondary tasks of robot control.

variability, and velocity as dance step features impacting on audience experience. In their studies, both professional dancers and inexperienced male dancers were involved.

The recent trend of augmenting traditional choreographies and common performances with artifacts has fostered new research about additional parameters of inanimate actors impacting the spectator's judgments [10], [11]. The research on robotic dance has focused more on the performances of humanoid or quadrupedal robots and drone swarms [12]–[14]. This has been aimed at demonstrating the impact and benefits of robot choreographies on human society providing *i*) novel forms of human-robot interaction [15], [16], *ii*) nonverbal communication for exchanging intentions between humans and non-human agents [17]–[19], *iii*) and psychological support during therapies for illnesses such as autism or other cognitive disabilities [20], [21]. Other research oriented to dissect the meaning of “beauty” for robotic movements has contributed to the field of artistic expressions [22]–[24], addressing a more conscious art-technologies integration and quantifying the impact of robotics on aesthetic experiences.

Despite the growing interest in aesthetic human-robot interaction and human-robot choreography, the projection of dancing human movements onto serial kinematic chains, such as robot manipulators, remains an open field to explore. The autonomous choreography generation through mapping can simplify the tasks of dancers and choreographers by offering *i*) a more natural language for communication with the robot, *ii*) the flexibility to rearrange the choreography in real-time during the performance, and *iii*) greater awareness of robot movements. Some relevant early works in this field include [25], in which Rogel *et al.* demonstrated the feasibility of mapping human dancing movement onto the robotic arm, or [26] and [27] proposing two approaches of reduction and mapping of human joint angles onto robotic arm chains. In [28] the authors explore the usage of data analysis methods to fit the mechanical movements of a robot with the space of the

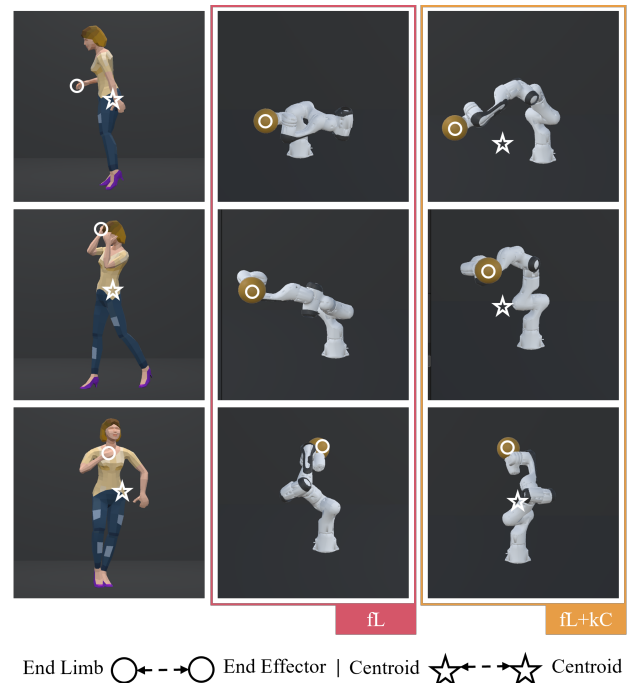


FIGURE 2: In each row, a representative example of the effects of the centroid alignment secondary task ( $kC+fL$ ) on the robot's posture is compared with the end-effector control on the position of the left upper limb ( $fL$ ) and human posture (from right to left). When following only the most variable limb, the robot may curl up as occurs in the first row, reach completely extended postures, hitting joint limits and consequently introducing positional error in the next dance steps (as noticeable in the second row), or, as visually depicted in the third row, exhibit body orientations dissimilar to those of the human. Including the keep-centroid task promotes more upright postures and human-like body orientations.

aesthetic movements of a dancer.

## B. CONTRIBUTION

Moving from the outcomes of above mentioned investigations about HRC generation by dancer mapping and leveraging our experience in the projection of human movements in both similar and dissimilar kinematic chains [29]–[31], in this work, we propose a multi-point method to project both dancing human posture and the nuance of artistic performance onto a robotic arm. To do this, we chose two representative geometrical points of the human kinematic chain: *i*) the centroid, and *ii*) the tip of the most variable end-limb (hand or foot) to map onto the robot center of gravity and its end-effector. That choice is based on two distinct hypotheses:

**Hp1** *The mapping of the dancer centroid onto the robot center of gravity ensures the posture imitation.*

The geometrical center of gravity of the dancer is the one of most representative points to describe the performer's balancing capability and, consequently, the reached posture during dance [32], [33].

**Hp2** *The mapping of the most variable limb of the dancer onto the robot end-effector ensures transmission of choreography nuance.*

According to the results of Torrents *et al.* and Neave *et al.* [8] and [9], reported before, wide movements impact positively on the audience experience, captivating the audience.

These hypotheses are also grounded on the relationship between perceived beauty, dancer emulation, and choreography expressiveness observed by authors in [26], wherein we noted a distinct polarization of opinions among users who preferred choreographies where the robot closely emulated the dancer's widest movements. In Fig. 2, the visual effects of the simultaneous mapping of most variable limbs and the posture of human dancers are depicted.

## II. METHOD

In what follows, we describe the human mapping method to simultaneously achieve the human-likeness of robot posture and expressiveness of robotic choreographies by following the most variable limb (fL) and keeping the human and robot centroids aligned (kC). Assuming to use a redundant robot ( $N \geq 7$ , with  $N$  amount of robot Degrees of Freedom, DoFs), we take advantage of the null space in its Jacobian matrix. The fL task is chosen as the primary one while the control of the dancer centroid path is projected in the robot kernel. In this way, wide and variable movements enable the end-effector movement while the whole robot kinematic chain attempts to keep a human-like posture. The desired joint angles  $q_{kC+fL}(t)$ , depends on this two tasks:

$$q_{kC+fL}(t) = q_{fL}(t) + q_{kC}(t) \quad (1)$$

where  $q_{fL}$  is the action in the joint space to follow the limb tip, while  $q_{kC}$  is the joint contribution to keep aligned the centroids of human and robot

In what follows, we detail both contributions  $q_{fL}$  and  $q_{kC}$  included in  $q_{kC+fL}$  robot joint space reference.

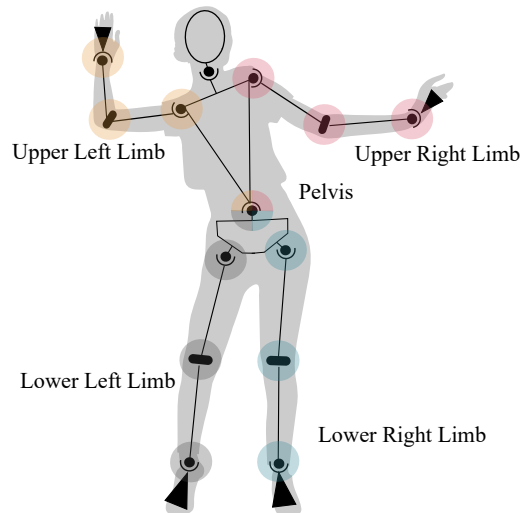


FIGURE 3: Human kinematic chains are generated by body segmentation in order to map the most variable end limb movement in the robotic arm for fL action.

### A. FOLLOW THE MOST VARIABLE LIMB (fL)

For what concerns the computation of fL action, the first step consists of identifying the set of human joints describing the position of the most variable limb. For this purpose, we segment the dancer's kinematic chain into four sub-chains with a common base: the pelvis point. As visually depicted in Fig. 3, we denote the resulting four kinematic chains as “upper left limb” (*ul*), “upper right limb” (*ur*), “lower left limb” (*ll*), and “lower right limb” (*lr*), containing the joint sub-set  $q_{h,ul}(t)$ ,  $q_{h,ur}(t)$ ,  $q_{h,ll}(t)$ , and  $q_{h,lr}(t)$ , respectively.

In order to evaluate the width of each kinematic chain movement, we also define a variance metric  $\varsigma_i$  as the time-based standard deviation of human kinematic ends:

$$\varsigma_{h,i} = \frac{1}{T} \sqrt{\int_T \left( \int_t^{t+\delta t} J_{h,i} \frac{\delta q_{h,i}(\tau)}{\delta \tau} d\tau \right)^2 - \bar{p}_{h,i}^2} dt$$

**with**  $i \in [ur, ul, lr, ll]$

Where  $T$  is the time to accomplish the choreography, while  $J_{h,i}$  is the Jacobian matrix of  $i$ -th kinematic chain relating the velocity at its extremity in the pelvis reference frame with the joint configuration, and  $\bar{p}_{h,i}(t)$  denotes the time-average of  $i$ -th kinematic chain tip position  $p_{h,i}$  as:

$$\bar{p}_{h,i} = \frac{1}{T} \int_T \underbrace{\left( \int_t^{t+\delta t} J_{h,i} \frac{\delta q_{h,i}(\tau)}{\delta \tau} d\tau \right)}_{P_{h,i}(t)} dt$$

**with**  $i \in [ur, ul, lr, ll]$

Once defined the most variable limb  $\tilde{i}$  as:

$$\tilde{i} = \arg \max_i (\varsigma_{h,i}) \quad \text{with } i \in [ur, ul, lr, ll]$$

its position is scaled by  $k_{h \rightarrow r}$  matrix and then projected onto the manipulator. The robot joint angles contribution  $q_{fL}(t)$

are evaluated on-line using a close loop differential inverse kinematics algorithm:

$$q_{fL}(t) = \int_t^{t+\delta t} J_r^\dagger \left( k_{h \rightarrow r} J_{h,i} \frac{\delta q_{h,\bar{i}}(\tau)}{\delta \tau} + K_c e_{ee}(\tau) \right) d\tau \quad (2)$$

<sup>1</sup> We use  $J_r \in \mathbb{R}^{6 \times N}$  to denote robot Jacobian matrix, while  $K_c$  is a  $\mathbb{R}^{6 \times 6}$  positive diagonal matrix that ensure the convergence of error  $e \in \mathbb{R}^6$ , defined as:

$$e_{ee} = p_{h,\bar{i}} - f_{fkine}(q_{fL})$$

where  $f_{fkine}(\cdot)$  is the forward kinematic function of robot.

### B. KEEP THE CENTROIDS ALIGNED (KC)

While the following of most variable end limb is evaluated as the primary task of the robot, the alignment of centroid action, kC, is computed as a secondary task exploiting the null space of the robot Jacobian matrix. This approach, according as described in [34], is commonly used to guarantee the accurate accomplishment of the primary task and achieve, simultaneously, additional tasks such as joint limit avoidance [35] or maximize the kinesthetic manipulability measure [36], [37] or also a combination of these [38]. Usually, exploiting the null space to accomplish a secondary task means projecting the gradient of a cost scalar function  $C(q) : \mathbb{R}^N \rightarrow \mathbb{R}$ , differentiable with respect  $q$ , to optimize it (minimize or maximize):

$$\dot{q}_{kC} = - \underbrace{(I_{N \times N} - J_r^\dagger J_r)}_{\mathcal{N}_{J_r}} \nabla_q C(q).$$

where  $\mathcal{N}_{J_r} = (I_{N \times N} - J_r^\dagger J_r)$  is the  $N \times N$  matrix projecting the gradient of cost function  $\nabla_q C(q)$  onto the null space of the Jacobian matrix  $J_r$ .

In this context, the optimization performed in the Jacobian null space comprises two weighted contributions: the primary contribution, denoted as  $B(q)$ , aims to minimize the distance between the human center of gravity, mapped into the robot workspace, and the robot's one, and an additional contribution,  $L(q)$ , aims to maximize the distance from the joint limits to prevent the robot from reaching these limits during its movements:

$$C(q) = \alpha B(q) + \beta L(q)$$

$\alpha$  and  $\beta$  are scaling factors that appropriately weigh each contribution to the overall cost.

To compute the  $B$  contribution, the first step is the evaluation of the dancer's center of gravity position  $c_h(t) = [x_{c,h}, y_{c,h}, z_{c,h}] \in \mathbb{R}^3$  as the centroid of  $M$  noticeable points  $p_{h,i}(t) \in \mathbb{R}^3$  with  $i \in [1, M]$  of human kinematic chain referenced to the pelvis point position  $\wp_h(t) \in \mathbb{R}^3$ :

$$c_h(t) = \frac{1}{M} \left( \sum_{i=1}^M p_{h,i}(t) \right) - \wp_h(t)$$

<sup>1</sup>We use the operator  $(\cdot)^\dagger$  to denote the pseudo-inversion operation.

Once evaluated  $c_h$ , it is scaled in the robot workspace to obtain the target position for the manipulator:

$$c_t(t) = k_{h \rightarrow r} c_h(t)$$

At the same time, the joint configuration of robot  $q(t) \in \mathbb{R}^N$  is used to compute its center of gravity  $c_r(t) = [x_{c,r}, y_{c,r}, z_{c,r}]$  as follows:

$$c_r(t) = \frac{1}{N} \left( \sum_{i=1}^N {}^0A_i(q_0(t), \dots, q_i(t)) \right) \begin{bmatrix} 0_{3 \times 1} \\ 1 \end{bmatrix} \quad (3)$$

where  ${}^0A_i \in \mathbb{R}^{4 \times 4}$  is the transformation matrix from  $i$ -th joint reference system to the base one. Then the resulting  $B$  contribution can be formulated as follows:

$$B(q) = \|c_t - c_r\|_2,$$

having  $\|\cdot\|_2$  that denotes the Euclidian distance expressed as  $\ell_2$  norm of difference of  $c_t$  and  $c_r$  vectors. Subsequently, according to (3), its differentiation respect to  $q$  values is equal to:

$$\nabla B = \frac{1}{N} \frac{(c_t - c_r)^T}{\|c_t - c_r\|_2} \nabla c_r$$

$$\text{with } \nabla c_r = \begin{bmatrix} \sum_{i=1}^N \frac{\partial x_i}{\partial q_1} & \dots & \sum_{i=n}^N \frac{\partial x_i}{\partial q_n} & \dots & \frac{\partial x_i}{\partial q_N} \\ \sum_{i=1}^N \frac{\partial y_i}{\partial q_1} & \dots & \sum_{i=n}^N \frac{\partial y_i}{\partial q_n} & \dots & \frac{\partial y_i}{\partial q_N} \\ \sum_{i=1}^N \frac{\partial z_i}{\partial q_1} & \dots & \sum_{i=n}^N \frac{\partial z_i}{\partial q_n} & \dots & \frac{\partial z_i}{\partial q_N} \end{bmatrix}$$

$x_i, y_i, z_i$  indicate the x, y, and z coordinates of the  $i$ -th joint, respectively, with  $i$  increasing from the base to the end-effector of the manipulator.

On the other hand, the preventing joint limits contribution  $L(q)$  is defined as proposed in [35]:

$$L(q) = \sum_{i=1}^N \left( \frac{1}{w_M - w(q_i)} - \frac{1}{w_M} \right)$$

being  $w(q_i)$  equal to:

$$w(q_i) = \left( \frac{q_i - \bar{q}_i}{q_{iM} - q_{im}} \right)^2 \quad (4)$$

with  $q_{iM}$  and  $q_{im}$  are the upper and lower joint limits, respectively, while  $\bar{q}_i$  represents the midpoint of the joint range. The term  $w_M = \frac{1}{4}$  is the maximum value that the (4) can assume. Consequently, maximizing the distance between the angle joints and their limits guarantees the feasibility of robot motion.

### III. IMPLEMENTATION

To test, validate, and subsequently conduct user studies about the proposed mapping method, we implemented and simulated an HRC in a virtual environment using a digital model of a Franka Emika Research 3 Robot model (Franka Robotics, GmbH), having  $N=7$ . We compared the performance of the proposed multi-point mapping with the robot tasked to accomplish single fL and kC actions. All values assumed by a mathematical parameter of the proposed mapping method are reported in Tab. 1.

N	M	T	$\delta t$	$k_{h \rightarrow r}$	$K_c$	$\tilde{i}$	$\alpha$	$\beta$
#	#	[mm:ss]	s	-	-	-	-	-
7	22	02:10	0.05	0.476	1	ur	0.9	0.1

TABLE 1: Parameters values used for the practical implementation of the proposed mapping method.

Limbs:	Upper Left	Upper Right	Lower Left	Lower Right
$s_{h,i}$	0.1899	<u>0.237</u>	0.0976	0.1018

TABLE 2: Results of variance analysis of dancer limbs on the recorded choreography. The underlining is used to indicate the highest value in the table and subsequently the involved limb into  $q_{fl}$  computation.

### A. DANCER DATA COLLECTION AND ANALYSIS

A professional dancer was asked to perform a hip-hop choreography for the song ‘‘Loco’’ by Itzy, the song and the style, were chosen to stress the mapping methods. The lack of rigid vocabulary<sup>2</sup> and solid dance grammar<sup>3</sup> makes the HRC generation more challenging. An Xsens suit (Xsens Technologies BV, NDL) was used to track the dancer’s movements by measuring and reconstructing 22 angles of the human body joints around the 3-axis, using data from 17 3D-IMUs, placed on the dancer’s body. During the choreography, the dancer’s motion data was collected and post-processed, centering and filtering it through a third-order Savitzky–Golay filter to obtain a smoother and less noisy signal.

Meanwhile, we analyzed the variance of dancer data according to the preliminary steps of the fL action. The analysis of recorded choreography returned that the right upper limb was the most activated kinematic sub-chain and, consequently, the right hand was chosen as a reference for fL action. All resulting variance values are visually reported in Tab. 2.

### B. SIMULATION ENVIRONMENT

To visualize and compare the obtained choreographies we realized a virtual environment consisting of a digital stage created by the Unity graphic engine (Unity Technologies, US) and populated with two mock-ups of the robot and a rigged human avatar (as shown in Fig. 4). The Franka Emika Research 3 Robot model was exploited to implement the proposed mapping and method and the singles fL and kC actions, controlling the cartesian positions of its end-effector and geometrical centroid. The virtual mannequins of robot were realized starting from its 3D model and enhanced with a kinematic skeleton by rigging with the Blender graphic tool (Blender Foundation). The movements of the robot and the dancer were reproduced in the form of animations. The virtual robot and human dancer avatar were located on the

<sup>2</sup>Dance vocabulary consists of reachable basic posture and movements. It depends on performance style and genre.

<sup>3</sup>The term ‘‘grammar’’ is used in the field of dance to encompass various elements forming the language of dance, including: body posture, rhythm, proximity relationship, gestures, and body direction and planes

	kC	fL	kC+fL
<b>End-Effector</b>	0.026 ± 0.016	0.013 ± 0.016	0.005 ± 0.005
<b>Centroid</b>	0.056 ± 0.062	0.331 ± 0.093	0.254 ± 0.118

TABLE 3: Summary of mean and variance of Euler error norm in the three actions.

virtual stage and recorded to perform a comparative user study between the proposed mapping method and consisting actions.

### C. VALIDATION

For the purpose of validating the functioning of the consisting contribution of control action and whole mapping method, we conducted a comparative analysis against individual implementations of the fL action within the same environmental conditions and using the same human data (see Fig. 5). Firstly, we examined the accuracy of following the end-effector when employing the fL+kC method, comparing it to movements generated by means of the fL action. In this case, the end-effector positioning error not only remained consistent and irrespective of the introduction of the kC action but also significantly decreased with respect to end-effector positioning error without kC contribution. In fact, the mean error reduction percentage  $\Delta\% \bar{e}_{ee,fL+kC}$ , evaluated as function of time-averaged values of end-effector positioning errors when fL+kC and fL contributions are exploited ( $\epsilon_{ee,fL+kC}$  and  $\epsilon_{ee,fL}$ , respectively):

$$\Delta\% \bar{e}_{ee,fL+kC} = 100 \frac{\bar{e}_{ee,fL} - \bar{e}_{ee,fL+kC}}{\bar{e}_{ee,fL}} \quad (5)$$

is equal to  $\Delta\% \bar{e}_{ee,fL+kC} = 29.6\%$ . The performance increase can be due to two reasons:

- The kC contributions include the joint limit penalty function that moves the robot towards posture far from the joint singularities that can negatively affect the accuracy of end-effector positioning;
- The tracking of centroid fosters robot postures more upright instead of bent ones preserving good levels of manipulability.



FIGURE 4: The virtual scenario, consisting of a stage with a human avatar reproducing a recorded choreography dancing to ‘‘Loco’’ by Itzy, and two mock-up of Franka Emika Panda robots enabled by two of presented mapping methods.

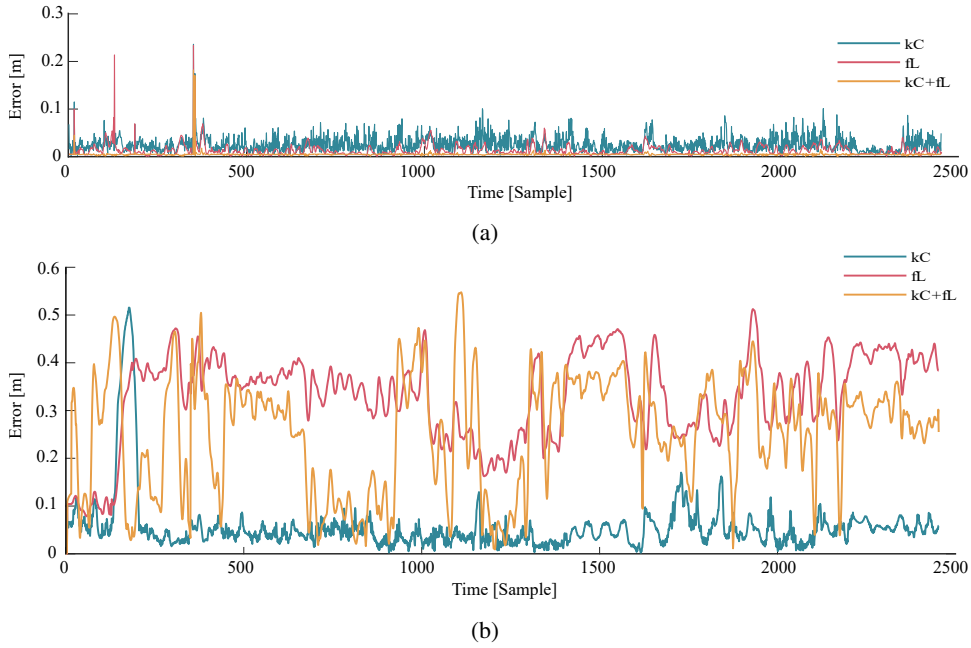


FIGURE 5: At the top (a), we present the  $\ell_2$  norm of the positional error with respect to the end effector target position for three proposed actions: fL, kC, and their combination. The bottom panel (b) illustrates the error norm relative to the centroid target position for the same actions.

In addition, we assessed the error reduction of centroid tracking when combining fL and kC with respect to using only the fL action. In this case, we observed an +23.26% increase in centroid following performance evaluated analogously to (5). Locally some centroid error increases occur. This lack of improvement is due to the online nature of the optimization method, which tries to optimize the robot pose without knowledge of the future desired. The robot reconfiguration in a certain time instant, aimed to minimize the cost function  $C(q)$ , moves it in a less advantageous posture for subsequent optimizations. A comprehensive summary of all quantified performances is presented in Table 3, detailing the average time errors relative to the path of human-mapped points and their standard deviation. For the sake of completeness also the performance of a kC control strategy obtained by inversion of (3) are added in Table 3.

#### IV. EXPERIMENTAL COMPARISON

An experimental investigation on emerging human-robot movement coherence and audience aesthetic perception of HRC was conducted to dissect the hypotheses outlined in Section I-B and measure the impact of the proposed mapping method on spectators. For this scope, the human collected data are analyzed and split to obtain six short phrases<sup>4</sup> each lasting  $15 \pm 3$  s. The duration of phrases aligns with that of typical social network content, ensuring a high level of engagement of people [39] involved during the user studies. Once again, human movements in phrases were used as references for robot

<sup>4</sup>In dance choreography, a phrase is a sequence of movements that make up a distinct and complete section of a dance.

control using the kC+fL method and both fL and kC single actions.

#### A. HUMAN-ROBOT COHERENCE

Firstly, the 18 resulting robot trajectories (six per two single control actions and the other six for the combined method) were analyzed to quantify the level of coherence between movement of the robot manipulator and the human. To do this, a joint-based approach was preferred to Cartesian one to mitigate the impact of the disparity in the length of links of two kinematic chains (the human and robot one) on the coherence measures. Following [28] and extending the methods proposed in [40] and [41], a preliminary visual inspection of the human-likeness of robot dance is conducted using the time-frequency maps obtained by  $(a, b)$ -weighted Wavelet continuous transformation  $W_{(\cdot)}$  and cross-wavelet spectrum  $W_{(\cdot),(\cdot)}$  measures:

$$D_w(\bar{q}_j, \bar{q}_{h,\bar{i}}) = \frac{|W_{(j)(h,\bar{i})}(a,b)|^2}{|W_{(j)}(a,b)|^2 |W_{(h,\bar{i})}(a,b)|^2} \quad (6)$$

**with**  $\forall j \in \{kC, fL, kC + fL\}$

and, subsequently, we exploited the cosine distance measure,  $D_c(\cdot, \cdot)$ , to quantify the dissimilarity of the movements, when robot accomplishes kC, fL, and kC+fL tasks, from the dancer:

$$D_c(\bar{q}_{h,\bar{i}}, \bar{q}_j) = 1 - \left| \frac{\int_0^T \bar{q}_{h,\bar{i}}(t) \bar{q}_j(t) \delta t}{\sqrt{(\int_0^T \bar{q}_j(t) \delta t)^2} \sqrt{(\int_0^T \bar{q}_{h,\bar{i}}(t) \delta t)^2}} \right| \quad (7)$$

**with**  $\forall j \in \{kC, fL, kC + fL\}$

When  $D_c(\cdot, \cdot)$  measure is near to zero, it indicates that movements are similar or one movement is nearly the opposite

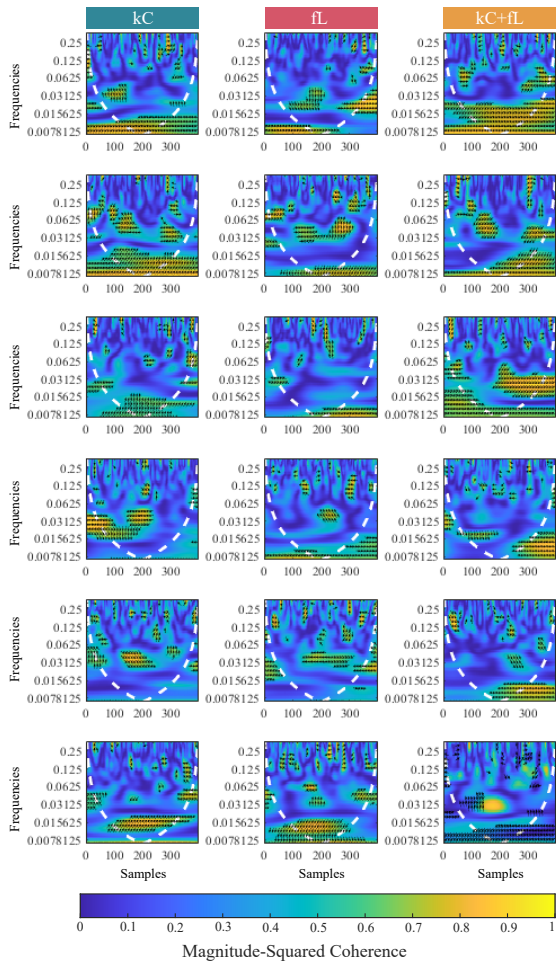


FIGURE 6: Time-frquence maps measured exploiting Wavelet coherence measure human dance and robot moving to accomplish kC, fL, kC+fL tasks (from left to right). Each raw consists of a single human-originating trajectory.

of the other. On the other hand, for values  $D_c(\cdot, \cdot) \approx 1$ , the two movements are poorly similar. In both (6) and (7),  $\bar{q}_{h,i}$  and  $\bar{q}_j$  denote the time series of average movements accomplished by human and robot in joint space, respectively, evaluated as:

$$\bar{q}_{h,i}(t) = \frac{1}{M} \sum_{m=1}^M q_{h,i,m}(t), \text{ and } \bar{q}_r(t) = \frac{1}{N} \sum_{n=1}^N q_{j,n}(t)$$

having  $q_{h,i,m}$  and  $q_{j,n}$  the angle measure of  $m$ -th and  $n$ -th joint of human and robot kinematic chains, respectively. The leveraging of this synthetic information about the joint state of both dancing actors was already explored in [28] to overcome the disparities of joint amount and DoF between the robot and human kinematic chains.

### 1) Results

From the preliminary examination of the Wavelet coherence map presented in Fig. 6, we observed a significantly higher

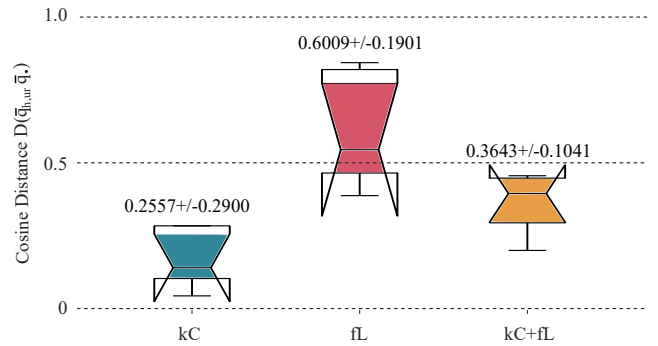


FIGURE 7: The levels of coherence measured as cosine distances  $D_c(\bar{q}_{h,ur}, \bar{q}_{kC})$ ,  $D_c(\bar{q}_{h,ur}, \bar{q}_{fL})$  and  $D_c(\bar{q}_{h,ur}, \bar{q}_{kC+fL})$  of human dance and robot movement generated exploiting the six phrases and the kC, fL actions and their combination, kC+fL, respectively.

level of similarity with the dancer's movements in the trajectories generated by controlling the centroid compared to those generated by controlling the end-effector. Additionally, an increase in coherence between the dancer's and the robot's movements is generally observed when comparing the trajectories generated by the fL and kC+fL control laws. Conversely, when comparing the trajectories generated by the kC and kC+fL control laws, the similarity to the human choreography is sometimes higher in the kC cases and at other times in the kC+fL cases. The qualitative results derived from the inspection of time-frequency coherence maps have been substantiated by the comparative analysis of measured cosine distances. The highest level of similarity to the human dance was achieved by the robot when controlled at its center of gravity, with a cosine distance  $D_c(\bar{q}_{h,ur}, \bar{q}_{kC}) = 0.2557 \pm 0.29$ . In contrast, the greatest distance was observed when the robot was tasked solely with following the most variable end limb, having a cosine distance equal to  $D_c(\bar{q}_{h,ur}, \bar{q}_{fL}) = 0.6009 \pm 0.1901$ . Furthermore, projecting the kC action onto the Jacobian null space of a robot performing the fL task resulted in a marked improvement in similarity  $D_c(\bar{q}_{h,ur}, \bar{q}_{kC+fL}) = 0.3643 \pm 0.1041$ , representing a reduction of  $\approx 40\%$  compared to the same control without the kC secondary task. The visual representation of quantitative analysis by cosine distances is provided as boxplots in Fig. 7.

### B. AUDIENCE AESTHETIC IMPACT

Finally, we conducted a user study to collect and analyze the audience's judgment about the perceived capability to imitate the human during the choreography, as well as the aesthetic preferences between the proposed methods, and the perceived sense of beauty of the resulting movement. Following the experimental protocol outlined in [42], we conducted six direct comparisons between the trajectories obtained by means of the proposed mapping method and the individual action contributions, resulting in video content. A total of 18 short video clips were recorded from the virtual environment, notably, each action was featured in 12 out of the 18 videos. The control strategies were assigned to left and

right positions randomly for each video to reduce the bias of the users. The clips were used to set up the user study in the form of an online survey consisting of five items (**I.x**) per comparison, two multiple-choice questions, an open input field, and two Likert scales:

- I.1** - Which robot (left or right) imitates the dancer avatar best? If neither left nor right imitates better than the other, please choose neither option.
- I.2** - Although neither robot is imitating well, which (left or right) would you choose if you had to pick?
- I.3** - Please explain why you made the choice you did for the previous question. Be specific to this video.
- I.4** - Please rate from 1 to 8 the beauty of choreography performed by humans and left robots.
- I.5** - Please rate from 1 to 8 the beauty of choreography performed by humans and the right robot.

The first question asked participants to evaluate the robot **imitation** capability of dancer movements, choosing between three options: *Left*, *Right*, and *Neither*. The second item offered two options (*Left* or *Right*) to identify the most appreciated human-robot choreography, quantifying the **appeal** of the implemented control strategies. The third question allowed participants to talk freely about why they made their choices. The remaining is aimed to measure the **beauty** perceived by the audience looking at the resulting HRCs.

The survey was completed by 30 users (16 female, 11 male, and 3 non-binary, aged 24-61). The experiment protocol was compliant with the declaration of Helsinki: there were no risks of harmful effects on the subjects' health and they could interrupt the task at any time. Participants were tasked to observe the videos and answer the items of the survey. At the end of the survey, they are asked to report their level of attention, interest, and experience in the dance discipline. All participants completed the survey in less than 30 min, and the average attention and interest level, rated on a 10-point Likert scale (from "low" to "high"), was  $6.78 \pm 1.58$  and  $7.73 \pm 1.88$ , respectively. Most participants declared themselves as amateurs and spectators of the dance discipline. Only three participants admitted to having no interest in dance, while two participants claimed to be professional dancers.

## 1) Results

We use as evaluation metrics the number of participants' preferences in terms of perceived imitation capability and appeal (first and second survey items, respectively). Moreover, we evaluate the opinions about the beauty of choreographies using the outcomes of the last two survey items.

**Imitation** - What concerns the opinion about the imitative capability of the proposed mapping method, against the single actions *kC* and *fL*, we analyze the collected results for each comparison, as visually depicted in Fig. 8.a. The direct comparison showed a clear difference in the perceived ability to mime the movements of the dancer: the combined method, *kC+fL*, yielded a +42 % difference with respect to the *fL* approach, with an uncertainty rate of below 30%. Similarly,

when comparing *kC+fL* and *kC* action, a +42% difference was noted, but a higher uncertainty rate of 18%. In the comparison between *kC* and *fL*, a 35% difference in favour of the former was found, but with a high rate of uncertainty equal to 41% of "*Neither*" chosen by survey participants.

For a deeper understanding of the collected results, a statistical analysis was conducted on the rearranged recorded opinions for each method and by subject. The "*Neither*" was exuded. A one-way repeated measures ANOVA was conducted to determinate whether there were statistically significant differences between the perceived imitation capability of the proposed methods. There were no outliers in the data, as assessed by inspection of a boxplot in Fig. 9.a. Data passed the Jaquera-Bera normality test ( $p > 0.05$ ), and the assumption of sphericity was not violated, as assessed by Mauchly's test of sphericity. The ANOVA test reported that there were statistically significant differences between the methods ( $F = 204.31 > F_{crit} = 2.25 \times 10^{-32}$ ). Post hoc analysis with a Bonferroni adjustment revealed that: *i*) There was a statistically significant difference between actions *kC+fL* and *kC*, with a higher number of preferences for the first method (with an average amount of choices equal to  $8.0783 \pm 1.609$ ) compared to the latter ( $3.1102 \pm 1.0887$ ) with a p-value of  $p < 0.01$ ; *ii*) The average amount of choices increased of +4.9681 in the case of *kC+fL* mapping when compared with *fL* ( $1.6429 \pm 0.731$ ) with a p-value less than 0.01; *iii*) also between *kC* and *fL* actions a statistically significant difference aroused ( $p < 0.01$ ).

**Appeal** - Similarly, we conduct an analysis of the opinion about the appeals of approaches, analyzing each comparison and globally the answers of the users, the results are visually depicted in Fig. 8.b and Fig. 9.b, respectively. The comparison between *kC+fL* and *kC* revealed that combined mapping was preferred by most of the users, with a difference of +46% between the two methods. Additionally, comparing the *fL* action and the *kC+fL* method, the latter was significantly more appreciated by users, with a difference of 62%, while of *kC* and *fL* comparison returned a result of +26% for *fL*.

Given that the data had no outliers and passed the Jaquera-Bera normality test ( $p > 0.05$ ), and Mauchly's test of sphericity did not violate the assumption of sphericity, we conducted a one-way repeated measures ANOVA. This revealed that there were statistically significant differences between the appeal of mapping methods according to spectators' opinions ( $F = 65.93 > F_{crit} = 1.012 \times 10^{-17}$ ). The post hoc analysis with a Bonferroni adjustment returned that: *i*) The *kC+fL* and *kC* statistically differed in terms of appeal with a p-value of  $p < 0.01$  and an increase of average expressed preferences of +3.72 for the combined method ( $9.00 \pm 1.7847$ ); *ii*) The appeal recorded by survey in the *fL* action ( $5.28 \pm 1.8828$ ) differed with the *kC* action by +5.29 ( $3.71 \pm 1.6297$ ) with  $p < 0.01$ ; and *iii*) The comparison between *kC+fL* and *fL* was also statistically significant with a p-value less than 0.01 and a difference of +1.57 of mean expressed preferences.

**Beauty** - Finally, we analyzed the perceived beauty of choreography performed with the three different groups, in



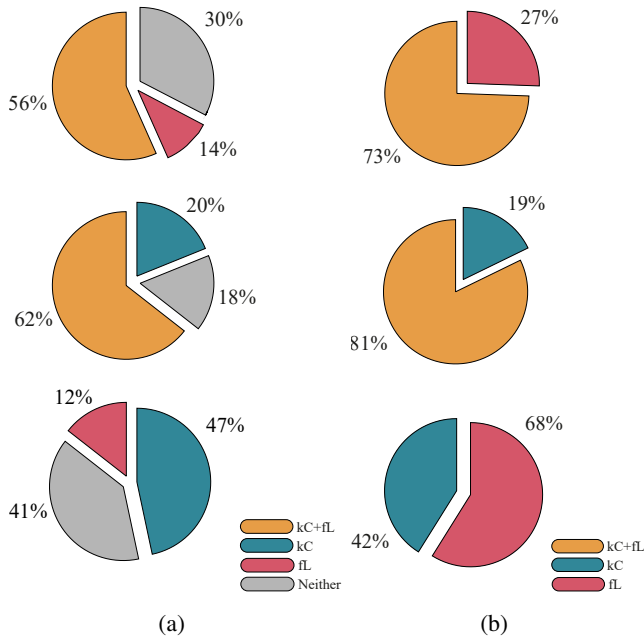


FIGURE 8: Results of the direct comparisons of collected users' opinions about perceived levels of imitation capability (a) and (b).

Fig. 9.c graphically reported the audience opinion distribution in histogram form. Due to the violation of the Jaquera-Bera normality test ( $p < 0.05$ ), we used a non-parametric test to study the difference between groups. The Kruskal Wallis ANOVA test revealed that there were statistically significant differences between the spectators' opinions ( $\chi^2 = 249.89$  and  $(p > \chi^2) = 5.45 \times 10^{-55}$ ). The post hoc multiple comparison analysis returned that there is a statistical difference among all groups with a p-value of  $p < 0.01$ , while a comparison of group median shows a +1 increasing beauty opinion from the kC contribution (median value equal to 3) to the fL one (median value equal to 4) and from fL to kC+fL (median value equal to 5) ones.

### C. DISCUSSIONS

In what follows we will provide a dissection of the initial hypothesis leveraging the outcomes of previous tests and the contents of choice explanation items of the survey.

**Hp1: The mapping of dancer centroids onto robot one ensures posture imitation** - According to the results of the analysis presented in Section IV-A1 the level of coherence between dancer and robot movement is highest when the latter is controlled to keep aligned its centroid with the human one. Moreover, performing this task in the null space of the robot improves its coherence with respect to the only tracking of the most variable link of the performer. On the basis of these observations, we can assess that the Hp1 is correct, then, that the human centroid is a good candidate point to synthesise the human posture. Subsequently, its mapping onto the robot ensures posture imitation and human-likeness of resulting

choreography. On the other hand, the findings of the user study suggest that the centroid-mapping approach was the least popular among users, despite audience judgments confirming its contribution to the similarity of human-robot movements, in fact, in these cases, they define the robot controlled only by kC contribution as “coordinated” (occurred 18 times), “in rhythm” (11), and “controlled” (5). It is interesting to note that users perceived the robot in the kC+fL case as more capable of imitating human movements compared to the kC case, even when numerical assessments of imitative ability suggested otherwise. To explore this phenomenon further, we interviewed several participants. They revealed that in many cases, the imitation capability of both robots was perceived as sufficiently high, making it difficult to choose “neither” as an option. As a result, when faced with this challenge, they tended to select the robot whose movements appeared more appealing. In essence, we can say that users' judgments of posture imitation were influenced by the gracefulness of the robot's movements when both robots exhibited a high level of coherence. Thus, the initial hypothesis that the centroid could effectively project the dancer's balance and posture was corroborated. Additionally, we demonstrated that combining this approach with another action, such as fL, which enhances the aesthetic appeal of the resulting choreography, further increases the perceived human-likeness of the movements.

**Hp2: The mapping of the most variable limb of the dancer onto the robot end-effector ensures the appeal of choreography** - The quantitative analysis of fL contribution did not return any information about expressiveness and appeal. Conversely, the results of the user study suggest that the fL action was preferred over kC one in terms of appreciation. Participants used terms such as “wider” (30 times), “expressive” (22) to motivate their preferences for this, indicating that they appreciated the broad movements. This suggests the greater expressive capability of the fL action, confirming the hypothesis that appealing to wider movements on audience opinions.

In the end, the kC+fL method results in a good trade-off ensuring the appeal of the fL contribution maintaining a high level of human similarity exploiting kC action as a secondary task for the robot. This makes the proposed method the most preferred one by users. Their preferences varied depending on what it was being compared to: when it was compared to kC alone action, in users' statements often occurred terms such as “wide” or “wider” (31 times), “expressive” (14), and “mobility” and “agile” (14). While, when comparing this method to the fL contribution, the most common terms used to justify the expressed preference were “similar” or “equal” (29), “synchronous” (09), and “moves as”, “like” (14), similarly to Hp1 dissertation. This indicates that users appreciated the similarity of the robot movements and the synchronization with the dancer when the combined method is used.

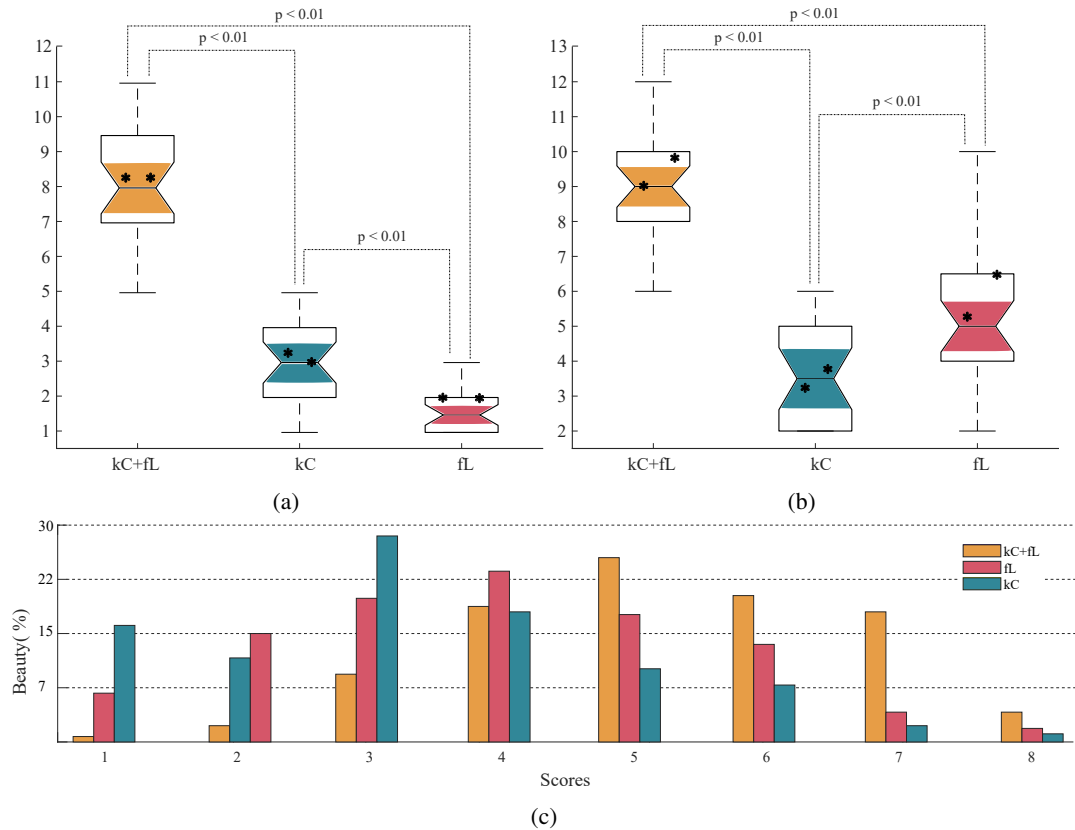


FIGURE 9: The number of collected preferences about perceived imitative capability and appeal is reported in (a) and (b), respectively. The p-values are reported on top of the boxes and the “\*” markers indicate the data collected from pro dancers. In (c), the histogram visually reports the audience’s opinion about the beauty of human-robot choreography.

## V. OPEN SCIENTIFIC QUESTIONS AND FUTURE WORKS

Despite the comprehensive experimental evaluation, several scientific questions remain unanswered. One open research question concerns the feasibility of the proposed method for the on-line generation of the HRC in realistic scenarios. The presence of humans on the same stage of the robot makes the environment highly unstructured. The robot control system must also prioritize the safety of dancers, avoiding collisions with them. Therefore, more complex control strategies than traditional kinematic-based ones should be implemented. We will compare the resulting performance of the same method here proposed implementing the kC action by means of an approach based on reinforcement learning to manage the human presence on the stage and reduce risks for the dancers.

We, also, plan to investigate how different forms of dance, from ballet to post-modern dance, are impacted by the strategy we have proposed, as well as the influence of robot kinematics on the aesthetic experience with different manipulators.

Moreover, in this context, aligning with the outcomes of previous studies on features impacting audience judgment, we propose a rigid strategy for selecting the limb reference for the fL action. However, we are aware that this approach reduces the expressive capability and decision space of the performer. To address these limitations, we plan to develop a user-driven

switching strategy that will restore the ability of dancers and choreographers to design the robot’s dance steps together with the autonomous algorithm. By integrating this shared control of the robot, we hope to balance the effectiveness of structured control and provide flexibility for artistic expression, providing a user-algorithm co-design platform.

## VI. CONCLUSIONS

In this study, we presented a new technique for creating human-robot dance choreographies based on multiple-point mapping from human to inhuman actors. We combine the projection of two dancers’ kinematic chain points onto the equivalent ones of the robot: the end of the most moved limb and the geometrical center of gravity. The first point is chosen to describe the high variability of the artistic performance while the latter represents the performer’s posture and balance. By exploitation of this method, we generated robot choreographies starting from human data acquisition, an example of these is visually depicted in a storyboard sequence of human and robot postures reported in Fig. 10 while a representative video clip of HRC is publicly available.<sup>5</sup>

<sup>5</sup>The video clip of the human-robot choreography generated by mapping both the end-limb and centroid of the dancer in the robot manipulator is uploaded on YouTube and reachable at the link: [https://youtu.be/T5h6fQ\\_73Ck](https://youtu.be/T5h6fQ_73Ck)

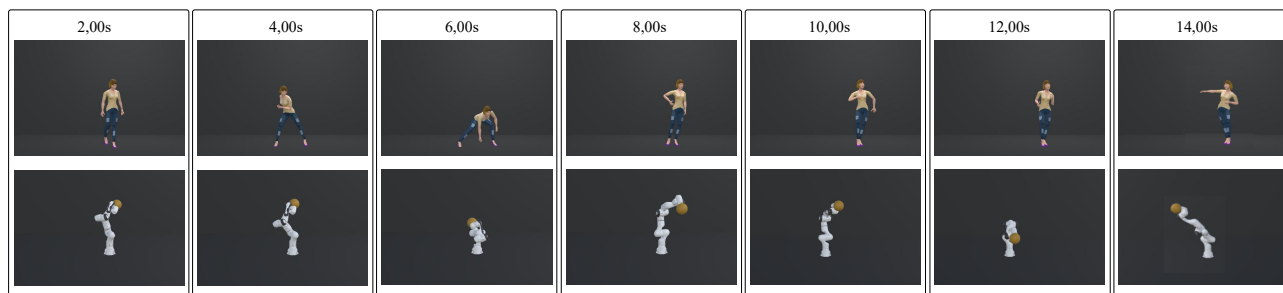


FIGURE 10: Storyboard sequences of continuous actions of human movements (first row) and robot performances (the last row) in a video clip generated exploiting the proposed points-to-points mapping strategy.

We conducted numerical validation and user studies to dissect the hypotheses on which the points are chosen and to evaluate the effectiveness of the proposed method. For this purpose, each consisting of control action and their combination were implemented on a virtual Franka Emika Panda robot in a simulated environment. According to the outcomes of human-coherence analysis, the *kC* action positively affects the similarity between the human and mechanical actors in the scene, while the *fL* action fosters the expressiveness of the resulting choreographies impacting the appeal of these. Subsequently, the proposed method mix efficiently the positive effects hypothesized for each point mapping, as confirmed by the opinion of the user studies participants and the similarity conducted analysis.

This research will be a significant step towards creating augmented aesthetic experiences in both the virtual and physical world through the mapping of human movement in reduced kinematic chains.

## REFERENCES

- [1] B. Calvo-Merino, C. Jola, D. E. Glaser, and P. Haggard, "Towards a sensorimotor aesthetics of performing art," *Consciousness and cognition*, vol. 17, no. 3, pp. 911–922, 2008.
- [2] M. Merritt, "Merritt robot dance," 2020. [Online]. Available: <https://www.youtube.com/watch?v=uSOHc3ODLzU>
- [3] R. Bolle, "l'uomo e la macchina," 20219. [Online]. Available: <https://www.youtube.com/watch?v=XH8C0i51ezk>
- [4] BostonDynamics, "Spot's on it," 2021. [Online]. Available: [https://www.youtube.com/watch?v=vQ-c\\_y31LU&t=6s](https://www.youtube.com/watch?v=vQ-c_y31LU&t=6s)
- [5] B. Click, "The robot and the ballerina," 2021. [Online]. Available: <https://www.youtube.com/watch?v=7atZfX85nd4>
- [6] E. Ackerman, "Ieespectrum - how boston dynamics taught its robots to dance aaron saunders, boston dynamics' vp of engineering, tells us where atlas got its moves from," 2021. [Online]. Available: <https://spectrum.ieee.org/how-boston-dynamics-taught-its-robots-to-dance>
- [7] H. J. Eysenck, "The general factor in aesthetic judgements 1," *British Journal of Psychology. General Section*, vol. 31, no. 1, pp. 94–102, 1940.
- [8] C. Torrents, M. Castaner, T. Jofre, G. Morey, and F. Reverter, "Kinematic parameters that influence the aesthetic perception of beauty in contemporary dance," *Perception*, vol. 42, no. 4, pp. 447–458, 2013.
- [9] N. Neave, K. McCarty, J. Freynik, N. Caplan, J. Honekopp, and B. Fink, "Male dance moves that catch a woman's eye," *Biology letters*, vol. 7, no. 2, pp. 221–224, 2011.
- [10] C. Breazeal and B. Scassellati, "Robots that imitate humans," *Trends in cognitive sciences*, vol. 6, no. 11, pp. 481–487, 2002.
- [11] D. O. Johnson and R. H. Cuijpers, "Investigating the effect of a humanoid robot's head position on imitating human emotions," *International Journal of Social Robotics*, vol. 11, pp. 65–74, 2019.
- [12] M. Fujita, K. Sabe, Y. Kuroki, T. Ishida *et al.*, "Sdr-4x ii: A small humanoid as an entertainer in home environment," in *Robotics Research. The Eleventh International Symposium*. Springer, 2005, pp. 355–364.
- [13] S. Nakaoka, A. Nakazawa, K. Yokoi, and K. Ikeuchi, "Leg motion primitives for a dancing humanoid robot," in *IEEE International Conference on Robotics and Automation, 2004. Proceedings. ICRA'04. 2004*, vol. 1. IEEE, 2004, pp. 610–615.
- [14] T. Schulz, J. Torresen, and J. Herstad, "Animation techniques in human-robot interaction user studies: A systematic literature review," *ACM Transactions on Human-Robot Interaction (THRI)*, vol. 8, no. 2, pp. 1–22, 2019.
- [15] M. Vircikova and P. Sincak, "Dance choreography design of humanoid robots using interactive evolutionary computation," in *Proceedings of the 3rd Workshop for Young Researchers on Human-Friendly Robotics (HFR 2010)*, Tübingen, Germany, 2010, pp. 28–29.
- [16] M. Vircikova, Z. Fedor, and P. Sincak, "Design of verbal and non-verbal human-robot interactive system," in *2011 11th IEEE-RAS International Conference on Humanoid Robots*. IEEE, 2011, pp. 87–92.
- [17] A. Beck, L. Cañamero, A. Hiolle, L. Damiano, P. Cosi, F. Tesser, and G. Sommavilla, "Interpretation of emotional body language displayed by a humanoid robot: A case study with children," *International Journal of Social Robotics*, vol. 5, no. 3, pp. 325–334, 2013.
- [18] D. McColl and G. Nejat, "Recognizing emotional body language displayed by a human-like social robot," *International Journal of Social Robotics*, vol. 6, no. 2, pp. 261–280, 2014.
- [19] S. Yoshida, D. Sakamoto, Y. Sugiura, M. Inami, and T. Igarashi, "Robo-jockey: robotic dance entertainment for all," in *SIGGRAPH Asia 2012 Emerging Technologies*, 2012, pp. 1–2.
- [20] B. Robins, K. Dautenhahn, E. Ferrari, G. Kronreif, B. Prazak-Aram, P. Marti, I. Iacono, G. J. Gelderblom, T. Bernd, F. Caprino *et al.*, "Scenarios of robot-assisted play for children with cognitive and physical disabilities," *Interaction Studies*, vol. 13, no. 2, pp. 189–234, 2012.
- [21] G. Bird, J. Leighton, C. Press, and C. Heyes, "Intact automatic imitation of human and robot actions in autism spectrum disorders," *Proceedings of the Royal Society B: Biological Sciences*, vol. 274, no. 1628, pp. 3027–3031, 2007.
- [22] M. Apostolos, M. Littman, S. Lane, D. Handelman, and J. Gelfand, "Robot choreography: An artistic-scientific connection," *Computers & Mathematics with Applications*, vol. 32, no. 1, pp. 1–4, 1996.
- [23] H. Peng, C. Zhou, H. Hu, F. Chao, and J. Li, "Robotic dance in social robotics—a taxonomy," *IEEE Transactions on Human-Machine Systems*, vol. 45, no. 3, pp. 281–293, 2015.
- [24] M. Apostolos, "Robot choreography: An aesthetic application in user acceptance of a robotic arm," in *Proceedings. 1986 IEEE International Conference on Robotics and Automation*, vol. 3. IEEE, 1986, pp. 753–756.
- [25] A. Rogel, R. Savery, N. Yang, and G. Weinberg, "Robogroove: Creating fluid motion for dancing robotic arms," in *Proceedings of the 8th International Conference on Movement and Computing*, 2022, pp. 1–9.
- [26] G. Saviano, A. Villani, and D. Prattichizzo, "A pca-based method to map aesthetic movements from dancer to robotic arm," in *2023 IEEE International Conference on Advanced Robotics and Its Social Impacts (ARSO)*, 2023, pp. 71–77.
- [27] M.-c. Wang and Y.-T. Shen, "An intuitive human-robot interaction method for robotic dance choreography," in *International Conference on Human-Computer Interaction*. Springer, 2023, pp. 248–257.

[28] G. Saviano, A. Villani, and D. Prattichizzo, "From cage to stage: Mapping human dance movements onto industrial robotic arm motion," in *Proceedings of the 9th International Conference on Movement and Computing*, ser. MOCO '24. New York, NY, USA: Association for Computing Machinery, 2024. [Online]. Available: <https://doi.org/10.1145/3658852.3659090>

[29] F. Ficuciello, A. Villani, T. L. Baldi, and D. Prattichizzo, "A human gesture mapping method to control a multi-functional hand for robot-assisted laparoscopic surgery: The musha case," *Frontiers in Robotics and AI*, vol. 8, 2021.

[30] T. L. Baldi, N. D'Aurizio, A. Villani, and D. Prattichizzo, "Generating kinesthetic feedback using self contact and velocity scaling," in *2021 IEEE World Haptics Conference (WHC)*. IEEE, 2021, pp. 619–624.

[31] A. Villani, G. Cortigiani, B. Brogi, N. D'Aurizio, T. L. Baldi, and D. Prattichizzo, "Avatarm: an avatar with manipulation capabilities for the physical metaverse," in *2023 IEEE International Conference on Robotics and Automation (ICRA)*, 2023, pp. 11 626–11 632.

[32] A. D. Kuo and F. E. Zajac, "Human standing posture: multi-joint movement strategies based on biomechanical constraints," *Progress in brain research*, vol. 97, pp. 349–358, 1993.

[33] E. Yu and J. K. Aggarwal, "Human action recognition with extremities as semantic posture representation," in *2009 IEEE Computer Society Conference on Computer Vision and Pattern Recognition Workshops*. IEEE, 2009, pp. 1–8.

[34] L. V. B. Siciliano, L. Sciavicco and G. Oriolo, *Robotics: Modelling, Planning and Control*. Springer Publishing Company, Incorporated, 2010.

[35] A. Liegeois *et al.*, "Automatic supervisory control of the configuration and behavior of multibody mechanisms," *IEEE transactions on systems, man, and cybernetics*, vol. 7, no. 12, pp. 868–871, 1977.

[36] T. Yoshikawa, "Manipulability of robotic mechanisms," *The international journal of Robotics Research*, vol. 4, no. 2, pp. 3–9, 1985.

[37] —, "Dynamic manipulability of robot manipulators," in *Proceedings. 1985 IEEE International Conference on Robotics and Automation*, vol. 2, 1985, pp. 1033–1038.

[38] F. Chen, M. Selvaggio, and D. G. Caldwell, "Dexterous grasping by manipulability selection for mobile manipulator with visual guidance," *IEEE Transactions on Industrial Informatics*, vol. 15, no. 2, pp. 1202–1210, 2018.

[39] X. Liang, X. Tao, and Y. Wang, "Impact analysis of short video on users behavior: Users behavior factors of short videoevidence from users data of tik tok," in *2021 7th International Conference on E-Business and Applications*, 2021, pp. 18–24.

[40] J. François, G. Messegue-Brocail, and F. Bevilacqua, "Movement analysis and decomposition with the continuous wavelet transform," in *Proceedings of the 8th International Conference on Movement and Computing*, 2022, pp. 1–13.

[41] E. Napier, G. Gray, and S. Oore, "Spectral analysis for dance movement query and interpolation," in *Proceedings of the 8th International Conference on Movement and Computing*, 2022, pp. 1–7.

[42] R. Kaushik and A. LaViers, "Imitation of human motion by low degree-of-freedom simulated robots and human preference for mappings driven by spinal, arm, and leg activity," *International Journal of Social Robotics*, vol. 11, pp. 765–782, 2019.



**ALBERTO VILLANI** (Student Member, IEEE) received the B.Sc. and M.Sc. degree cum laude in Automation Engineering in 2017 and 2020 from the University of Naples, Italy. He is currently pursuing a Ph.D. degree in robotics and automation with the Department of Information Engineering and Mathematics, University of Siena. His research interests include robotics and haptics focusing on human- and cell-centered robotics.



**DOMENICO PRATTICHIZZO** (Fellow, IEEE) received the M.S. degree in electronics engineering and the Ph.D. degree in robotics and automation from the University of Pisa, Pisa, Italy, in 1991 and 1995, respectively. He is a Professor of robotics with the University of Siena, Siena, Italy, and since 2009, a Scientific Consultant with Istituto Italiano di Tecnologia, Genova, Italy. In 1994, he was a visiting scientist with the MIT AI Lab. He has authored more than 200 papers in his research fields.

His main research interests include haptics, grasping, visual servoing, mobile robotics.

...



**GIUSEPPE SAVIANO** (Student Member, IEEE) received the B.Sc. and M.Sc. degree cum laude in Biomedical Engineering from the University of Naples (UNINA), Italy, in 2018 and 2021, respectively. He is currently pursuing a Ph.D. degree in AI&Society applied to robotic systems at the University of Siena. His research interests include investigating AI and Data analysis strategies tailored for mapping complex human movements within robotic systems.